Experimental/Analytical Evaluation of the Effect of Tip Mass on Atomic Force Microscope Calibration

Matthew S. Allen,[1] Hartono Sumali[2] & Elliott B. Locke[3]

[1]Assistant Professor, University of Wisconsin-Madison, 535 ERB, 1500 Engineering Drive, Madison, WI 53706, Corresponding Author: msallen@engr.wisc.edu

[2]Principal Member of Technical Staff, Sandia National Laboratories[1] P.O. Box 5800, Albuquerque, NM 87185, hsumali@sandia.gov

[3]Undergraduate Student, University of Wisconsin-Madison

Abstract:

Quantitative studies of material properties and interfaces using the atomic force microscope (AFM) have important applications in engineering, biotechnology and chemistry. Emerging studies require an estimate of the stiffness of the probe so that the forces exerted on a sample can be determined from the measured displacements. Numerous methods for determining the spring constant of AFM cantilevers have been proposed, yet none accounts for the effect of the mass of the probe tip on the calibration procedure. This work demonstrates that the probe tip does have a significant effect on the dynamic response of an AFM cantilever by experimentally measuring the first few modes of a commercial AFM probe and comparing them with those of a theoretical model for a cantilever probe that does not have a tip. The mass and inertia of an AFM probe tip are estimated from scanning electron microscope images and a simple model for the probe is derived and tuned to match the first few modes of the actual probe. Analysis suggests that both the method of Sader and the thermal tune method of Hutter and Bechhoefer give erroneous predictions of the area density or the effective mass of the probe. However, both methods do accurately predict the static stiffness of the AFM probe due to the fact that the mass terms cancel so long as the mode shape of the AFM probe does not deviate from the theoretical model. The calibration errors that would be induced due to differences between mode shapes measured in this study and the theoretical ones are estimated.

1. Introduction

The Atomic Force Microscope (AFM) has long since proved its utility for imaging at very small scales [1]. In recent years, effort has shifted towards obtaining quantitative information regarding material properties, friction, bond strengths, etc… at the nanoscale using the AFM. A number of procedures have been proposed to find the stiffness of the AFM cantilever so that the forces applied to a sample can be obtained from deflection measurements [2-7]. All of the methods available in the literature neglect the effect of the mass of the tip, which can be considerable compared to the mass of the cantilever beam on which it is mounted for many commercially available cantilevers. For example, Figure 1 shows scanning electron microscope (SEM) images of the tips of two micro cantilevers. Figure 2 shows an image of three cantilever beam AFM probes of the series studied here. The tip volume is significant relative to that of the beam, even for the long cantilevers shown in Figure 2.

This work evaluates the calibration error that is induced by neglecting the mass of the AFM tip, and seeks to derive more exact calibration procedures. The results presented here suggest that spring constant estimated by either the method of Sader [3] or the thermal tune method of Hutter and Bechhoefer [4] should be quite accurate, so long as the first elastic mode is used in the calibration. On the other hand, the effective mass (or area density) is greatly underestimated, the error being approximately proportional to the ratio of the tip mass to the effective mass of the cantilever, which is greater than 30% for the cantilever studied here. This work also estimates the magnitude of the error that can be incurred by using any of the higher modes of the cantilever to

[1] Sandia is a multiprogram laboratory operated by Sandia Corporation, a Lockheed Martin Company, for the United States Department of Energy's National Nuclear Security Administration under Contract DE-AC04-94AL85000.

perform the calibration. The results presented here reveal that special care must be taken when using higher harmonic imaging [8], because the higher modes are observed to be much more sensitive to the influence of the tip than the fundamental.

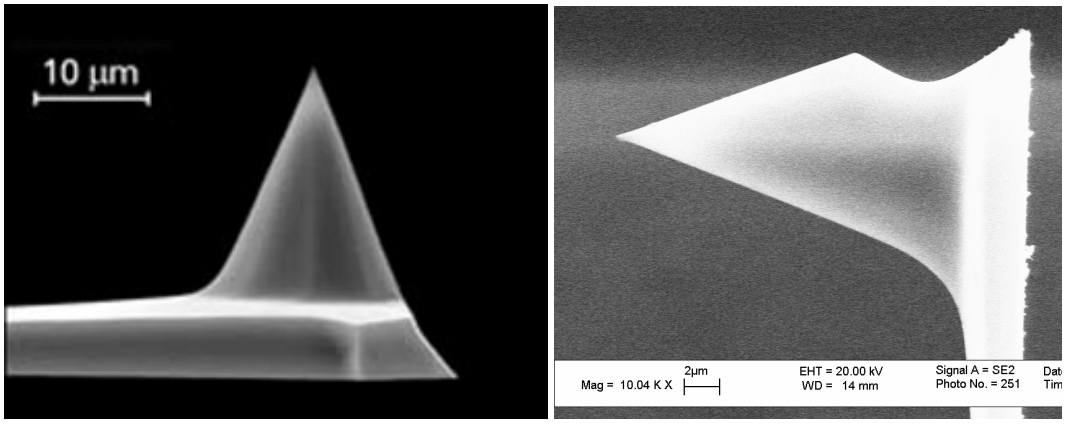

Figure 1: SEM images of AFM probe tips, (right) manufacturer's Image, (left) image of probe tip from the lot studied in this work.

In order to assess the importance of the tip to the dynamics of the AFM probe, the natural frequencies and mode shapes of a contact-mode AFM probe are measured and compared with those of a tip-less Euler-Bernoulli cantilever beam. The restraining effect of the tip is clearly visible. The mass and inertia of the tip are estimated from SEM images of a probe. A simple Ritz series model is then derived that includes the mass and inertia of the AFM tip, and the model is tuned to better mimic the dynamics of the first few bending modes of the AFM probe. Both the SEM estimated tip mass and that estimated from the calibrated model are used to find the error in the Sader prediction for the cantilever area density. The mode shapes of the tuned analytical model are also used to estimate the error in the stiffness predicted by the method of Sader.

2. AFM Calibration Procedures

Two of the most commonly used approaches for calibrating AFM cantilevers are the method of Sader [3] and the thermal tune method of Hutter & Bechhoefer [4]. The former derives an analytical model for the interaction of the cantilever with the surrounding fluid (typically air) and uses this to solve for the unknown density per unit area and stiffness of the cantilever from measurements of its resonance frequency and Q-factor in the fluid. The latter utilizes the equipartition theorem to find the cantilever's spring constant from the magnitude of its mean-square thermal vibration in air. A number of other, less commonly used procedures have also been proposed, including: applying nano-scale beads of known mass [5, 7] and using the AFM to deflect levers of known stiffness [6]. All of the methods that rely on a model for the cantilever have utilized an Euler-Bernoulli cantilever beam model and have neglected the effect of the probe-tip.

2.1. Calibration Method of Sader

Sader modeled the forces that a viscous fluid exerts on a vibrating cantilever beam in [9], showing that the fluid has both a mass loading and a vibration damping effect. The equation of motion for the surrounding fluid was solved and transformed to the frequency domain yielding the force F_{hydro} that the fluid applies to a differential cross section of the cantilever beam as a function of the beam's displacement $W(x,\omega)$, resulting in the following.

$$F_{hydro}\left(x,\omega\right)=\frac{\pi}{4}\rho_f\omega^2b^2\Gamma\left(\omega\right)W\left(x,\omega\right) \qquad (1)$$

The force that the fluid exerts on the beam depends on the fluid density ρ_f, the frequency ω of vibration, the beam's width b, and the hydrodynamic function $\Gamma(\omega)$. The hydrodynamic function is a complex function of frequency; its solution is given in [3, 9][2]. The solution assumes a long cantilever beam with rectangular cross section, whose width greatly exceeds its thickness. Sader then proceeded to find the solution for the forced

[2] One should note that the Bessel functions in the solution for the hydrodynamic function are Bessel functions of the second kind (hence the nomenclature K), not the third kind (Hankel functions) as stated in Sader's paper.

vibration of the cantilever in terms of Green's functions. The imaginary part of the hydrodynamic force, due to the imaginary part of $\Gamma(\omega)$, acts as a dissipative term, and is responsible for vibration damping. The real part acts as a mass term. Sader obtained analytical expressions for the Q-factor (or the damping ratio $\zeta = 1/(2Q)$) and the natural frequency ω_n of the cantilever vibrating freely in a fluid. He then recognized that these expressions could be solved for the area density $\rho_c h$ and static stiffness k_s of the cantilever as a function of the measured Q-factor and natural frequency, the in-plane dimensions of the cantilever, and the density and viscosity of the fluid. Sader's method has been used widely by probe manufacturers and experimentalists.

Sader's model can be modified to account for the effect of a tip on the cantilever beam by simply adding mass and inertia terms to the model. This is most easily done using a Ritz series model for the cantilever, and the result will be shown to reduce exactly to that presented by Sader using Greens functions, when the tip mass and inertial are zero. The Ritz method expresses the displacement at any point on the beam as a product of a spatial basis function $\psi(x)$ and a time function $y(t)$. For a single term series, one obtains the following frequency domain equation of motion for the amplitude $Y(\omega)$ of the Ritz basis function $\psi(x)$, and hence the response of the entire beam using $W(x,\omega) = \psi(x)Y(\omega)$.

$$-\omega^2\left[\left(\rho_c hbL+\frac{\pi}{4}\rho_f b^2 L\Gamma_r(\omega)\right)m_{11}+m_t\left(\psi(x_m)\right)^2+\frac{I_t}{L^2}\left(\frac{d}{dx}\psi(x_m)\right)^2\right]Y+$$
$$i\omega\left[\frac{\pi}{4}\rho_f \omega b^2 L\Gamma_i(\omega)m_{11}\right]Y+\left[\frac{k_s}{3}k_{11}\right]Y=0 \qquad (2),$$

$$\psi(x)=\sin(\alpha_1 x)-\sinh(\alpha_1 x)+R_1\left[\cos(\alpha_1 x)-\cosh(\alpha_1 x)\right]$$

$$m_{11}=\int_0^1\left(\psi(x)\right)^2 dx\approx 1.8556 \qquad (3),$$

$$k_{11}=\int_0^1\left(\frac{d^2}{dx^2}\psi(x)\right)^2 dx\approx 22.94$$

where ρ_c is the mass density of the cantilever, h and L are the height and length of the cantilever respectively, m_t is the mass of the tip, I_t its mass moment of inertia and x_m is the normalized location of the tip-mass (unity for the tip on the end of the cantilever). The static spring constant of the cantilever is k_s, which is equal to $E*bh^3/(4L^3)$ where E is the modulus of elasticity of the cantilever. The two constants R_1 = -1.3622 and α_1 = 1.8751. The terms m_{11} and k_{11} are the effective mass and effective stiffness of the cantilever. The text by Ginsberg [10] details how to implement the Ritz method for this type of analysis.

One can divide eq. (2) through by the mass factor and match the terms multiplying $i\omega Y$ and Y to $2\zeta\omega_n$ and ω_n^2 respectively to obtain analytical expressions for the damping ratio and natural frequency. One can then invert the procedure and solve for the area density $\rho_c h$ and the cantilever stiffness k_s from the parameters mentioned previously as well as the mass and inertia of the tip, resulting in the following expressions.

$$\rho_c h=\frac{\pi}{4}\rho_f b\left(\frac{1}{2\zeta}\Gamma_i(\omega)-\Gamma_r(\omega)\right)-\frac{m_t}{bLm_{11}}\left(\psi(x_m)\right)^2-\frac{I_t}{bL^3 m_{11}}\left(\frac{d}{dx}\psi(x_m)\right)^2 \qquad (4),$$

$$k_s=\frac{3\pi\rho_f b^2 L m_{11}\Gamma_i(\omega)}{4k_{11}}Q\omega_n^2 \qquad (5),$$

Equation (4) reduces exactly to the expression given by Sader and his colleagues in [3] if the tip mass and inertia are negligible. One can also verify that these equations agree with Sader's online calibrator[3] to within a small fraction of a percent. Interestingly, eq. (5) for the static stiffness is identical to that presented by Sader, even with the inclusion of the tip mass. The terms that include the tip mass and inertia have canceled!

The method of Sader implicitly assumes that the basis function $\psi(x)$, which is the first mode function of an Euler-Bernoulli beam, is a good approximation for first mode shape of the actual AFM probe. In general, on would expect that the inclusion of a significant tip mass would alter the shape of the modes of the probe. If the true mode shape differs from the assumed one, then a similar analysis employing the true mode function as the basis function results in the same equation for k_s (eq. (5)) with m_{11} and k_{11} replaced by the integrals of the true

[3] http://www.ampc.ms.unimelb.edu.au/afm/calibration.html#normal

mode functions. We denote the values of those integrals with hats, $\hat{m}_{11}$ and $\hat{k}_{11}$. Hence, we obtain the following relationship between the estimated spring constant k_s and the true one $k_{s,true}$

$$k_{s,true} = \frac{\hat{m}_{11}}{\hat{k}_{11}} \frac{k_{11}}{m_{11}} k_s \qquad (6),$$

This suggests that one can evaluate the accuracy of the method of Sader by comparing the true mode functions of an AFM with the analytical mode functions defined in eq. (3). This is done in for the probe of interest and discussed in the following section.

At this juncture, we note that one could apply this same procedure to any mode of the cantilever simply by replacing the terms m_{11} and k_{11} in the preceding equations with the integrals of the mode function for the desired mode (see eq. (3)). Such a procedure is useful when the fundamental mode cannot be accurately identified, or when higher-harmonic imaging is used [8].

2.2. Thermal Tune Calibration Method

A similar analysis reveals that the thermal tune method [4] also accurately predicts the static stiffness of the beam so long as the inclusion of the tip mass does not significantly alter the shape of the natural mode that is used in the calibration procedure. As with the method of Sader, one can estimate the accuracy of the thermal tune method by comparing the actual mode shapes with the theoretical ones. The thermal tune method does not accurately predict the effective mass of the cantilever if the tip mass is significant, even if the mode functions do not change shape.

3. Application to AFM Probe

The corrected method of Sader, which accounts for the tip mass, was applied to Mikromasch contact mode cantilevers of the 38th series. The manufacturer's specifications are shown below. The middle or "B" position cantilever from a few nominally identical chips was used for this study.

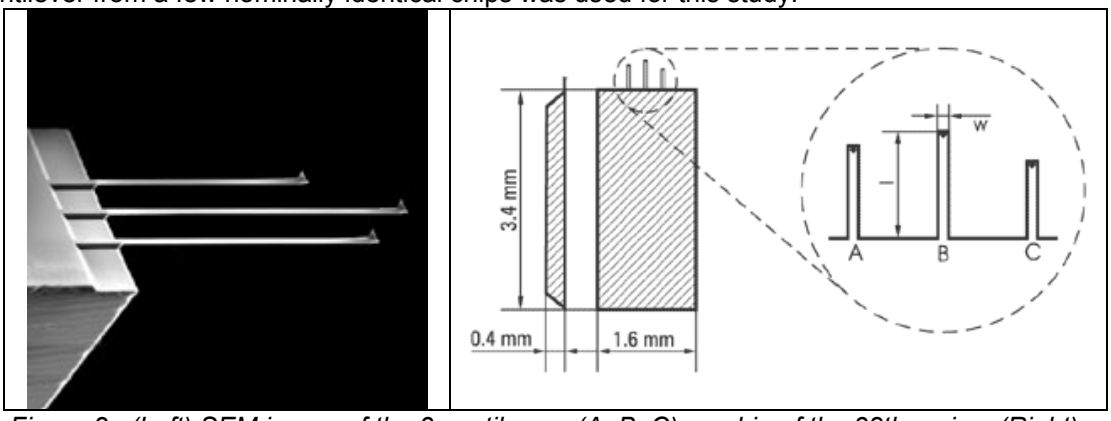

Figure 2: (Left) SEM image of the 3 cantilevers (A, B, C) on chip of the 38th series. (Right) Schematic of silicon chip of the 38th series showing 3 rectangular cantilevers.

Position	Cantilever Length ($l \pm 5$) μm	Cantilever Width ($w \pm 3$) μm	Cantilever Thickness (μm)			Resonant Frequency (kHz)			Force Constant (N/m)		
			min	typ	max	min	typ	max	min	typ	max
A	300	35	0.7	1.0	1.3	9.5	14	19	0.01	0.05	0.1
B	350	35	0.7	1.0	1.3	7.0	10	14	0.01	0.03	0.08
C	250	35	0.7	1.0	1.3	14	20	28	0.02	0.08	0.20

Table 1: Manufacturer specifications for AFM probes of the 38th series. The beam in the B position was used in this study.

3.1. Estimating Tip Mass and Inertia

The tip mass and inertia must be known to apply the corrected method of Sader in eqs. (4) and (5). An SEM image of a cantilever tip was obtained, shown in Figure 1, and was used to estimate the volume of the tip. The tip was approximated as a cone with base radius R_t and height L_t equal to 8.4 and 22.1 microns respectively. Using a nominal value for the density of silicon of ρ_t = 2300 kg/m^3 the mass of the tip is found to be m_t =

$\rho_t(\pi/3)L_tR_t^2$ = 3.76 ng. Assuming the same density for the cantilever and using the nominal dimensions in Table 1, the mass of the cantilever beam B was estimated to be m_b = 28.2 ng. Hence, the ratio of the tip mass to the total beam mass is 0.13. However, the effective mass of the cantilever, which is the important factor in dynamic calculations, is much less than its total mass of the beam. (The effective mass is the mass that would be applied to the tip of a massless beam to give the same effect as the actual mass, which is distributed along the length of the cantilever.) The effective mass is 25% of the total mass of the beam, estimated via eqs. (2-3), and also in [11]. The tip mass to effective mass ratio for this cantilever is 0.54. The mass moment of inertia of the tip, approximated as a cone, was found using the formula from Ginsberg [12] including the adjustment for the parallel axis theorem: $I_t = (3/80)m_t(4R_t^2+L_t^2+(L_t/4+h/2)^2)$.

There is considerable uncertainty associated with this calculation of the mass of the tip. First, observe that the image acquired for this work shows a tip that is far from a perfect cone, while the manufacturer supplied image is nearly conical. Second, note that the thickness of the cantilever beam is about 5μm near the tip, greatly exceeding the manufacturer's specification. Finally, one would expect that the density of the silicon from which the tip is made could vary considerably from its nominal value.

3.2. Experimental Validation

In order to verify that these values for the tip mass are reasonable, the first few modes of two cantilever AFM probes, both Mikromasch beam B of the 38th series, were measured using a Polytec MSV-400 Laser Doppler Vibrometer focused through a Mitutoyo optical microscope. The experimental procedure was essentially the same as that described in [13], and the tests were performed at low air pressures (~7mTorr) to minimize dissipation and hence improve the vibration signals. The first four operating deflection shapes and their peak frequencies were extracted from one beam at 7mTorr, and only the first two operating shapes from a second at ambient pressure. Considering the high quality factor of these modes, the operating shapes and the peak frequencies are very good approximations for the mode shapes and for the natural frequencies of the beams respectively. The natural frequencies of the first four modes (at very low air pressure) are reported in Table 2.

An analytical model of the probe was also created to compare with the experimental measurements. This analytical model consisted of a ten-term Ritz series [10] and included the effect of the mass and inertia of the tip as done in the single-term Ritz model in the previous section. Convergence of the Ritz series was verified by increasing its length to 50 terms and confirming that the mode shapes and natural frequencies of the first four modes did not change appreciably. The nominal dimensions for the cantilever (see Table 1) were used along with a nominal value for the modulus of silicon (E = 170 GPa) and the values given previously for the mass and inertia of the tip. The frequencies and mode shapes predicted by this initial model agreed roughly with those measured experimentally, yet there were significant differences.

The 1st, 2nd and 3rd natural frequencies of the model were affected quite strongly by the inclusion of the tip mass. However, one cannot use these to identify the tip mass in an absolute sense because there are various combinations of beam density, stiffness and tip mass that would give the same result. One can define a nondimensional factor for the beam as $(Ebh^3/(12L^3))/(\rho_c bhL)$, and obtain the same modal frequencies by adjusting this factor and the tip mass such that $m_t/(\rho_c bhL)$ remains constant. This ambiguity was circumvented by first optimizing based on the ratios of the 2nd and 3rd natural frequencies to the 1st. The model was optimized by varying the tip mass and its location x_m until the ratios of the 2nd and 3rd natural frequencies to the 1st matched very closely. It was also observed that this gave good agreement between the analytical mode shapes and the experimental ones. The nondimensional factor for the beam $(Ebh^3/(12L^3))/(\rho_c bhL)$ was then adjusted so that the first natural frequency exactly matched that of the experimental beam. This procedure uniquely identifies the nondimensional factor and the tip mass ratio $m_t/(\rho_c bhL)$ that give the best agreement between the model and experimental results.

One needs an estimate for either E, ρ_c or m_t to eliminate this ambiguity and determine unique values for the other two parameters. For the comparisons that follow, this was done by assuming that the static stiffness k_s = $(Ebh^3/(4L^3))$ estimated by the method of Sader, in the following section, was accurate. The beam density and the the mass of the tip could then be determined from the nondimensional factor $(Ebh^3/(12L^3))/(\rho_c bhL)$ and tip mass ratio $m_t/(\rho_c bhL)$. The resulting values are shown in Table 3.

The tip mass required to obtain good agreement with the model is more than twice that estimated from the SEM images. All of the other parameters are within a few percent of their nominal values. The resulting natural frequencies of the first four modes predicted by this model are shown in Table 2. The first three natural frequencies agree to within 2%, while the fourth is different by almost five percent.

Mode Number	Experimental (kHz)	Analytical (kHz)
1	9.07	9.07
2	70.8	70.5
3	213.8	210.3
4	439.8	419.8

Table 2: Natural frequencies of AFM probe measured experimentally and predicted analytically by Ritz model.

Parameter	Nominal Model	Tuned Model
$\mathbf{m_t}$	3.76 ng	8.0 ng
$\mathbf{x_m}$	1 (350 μm)	0.928 (325 μm)
$\mathbf{k_s}$	0.0414 N/m	0.0424 N/m
$\boldsymbol{\rho}$	2300 kg/m^3	2250 kg/m^3

Table 3: Nominal AFM probe parameters and parameters after tuning the model.

The first four mode shapes for the Ritz model are shown in Figure 3 along with the experimentally obtained operating shapes. The latter were rescaled to have the same norm as the analytical shapes for this plot. The analytical shapes agree quite well with the experimentally observed shapes, with a few exceptions. The tip motion for Beam 1 was considerably different than that of both Beam 2 and that of the analytical model for any reasonable value of the tip mass. A change of this order of magnitude of the first mode shape could have a significant effect on any calibration procedure, especially the thermal tune method since it relies on the mode shape near the tip matching the analytical mode function. Beam 1's second mode also agrees less closely with the second mode predicted by the analytical model than does Beam 2's, and its fourth mode shape also deviates significantly from the measurements near the tip end. While there is considerable uncertainty, the first two modes of the model do match the measured modes of Beam 2 quite well, and the third mode of the model matches the third mode of Beam 1 very well, so these modes can be used to evaluate the effect of the tip on the calibration methods.

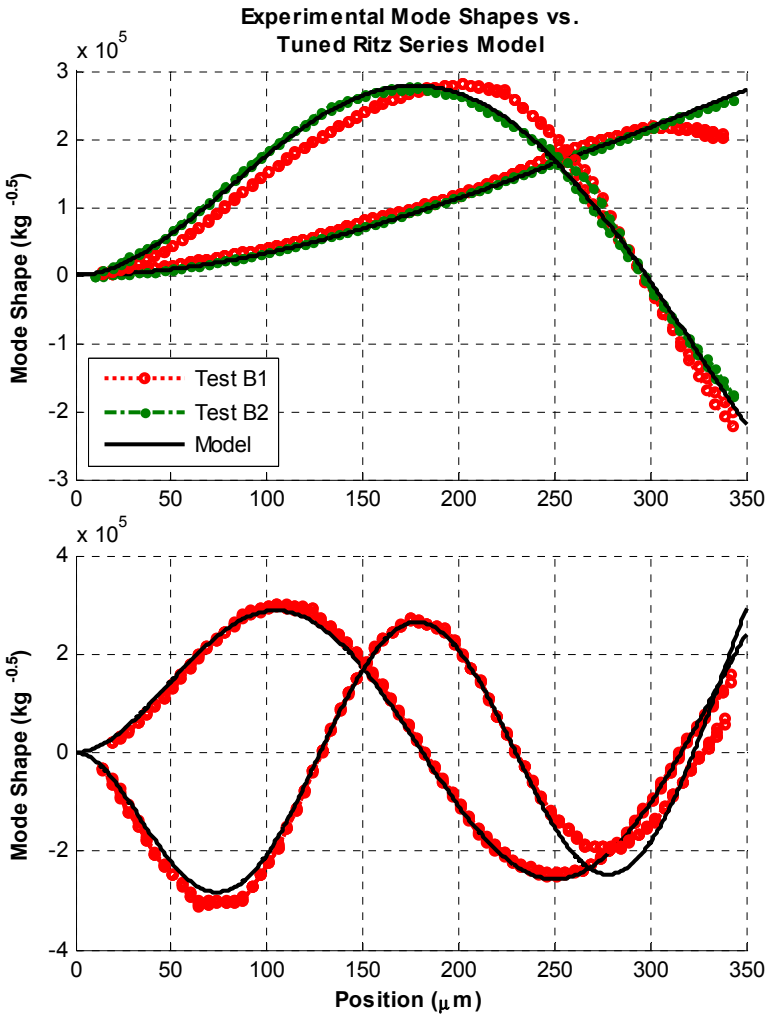

Figure 3: Experimentally measured mode shapes for two cantilever AFM probes (red and green) and mode shapes from a tuned Ritz model that includes the mass effects of the tip.

It has been noted in previous works that the inclusion of a sizable mass on the end of a cantilever beam does not significantly change either the shape of the first mode nor its effective stiffness significantly [11]. However, it is important to note that the effective mass of the beam, and hence the scale of the mode shape, does change considerably. This is illustrated in Figure 4, which shows the mass-normalized mode shapes for the cantilever probe both with and without the tip mass, as predicted by the tuned analytical model. The restraining effect of the tip mass is clearly evident near the end of the beam, where the mode shapes with the tip mass show considerably less motion due to the inclusion of the tip. The shape of the first mode does not change noticeably, yet its overall scale has reduced by 25%.

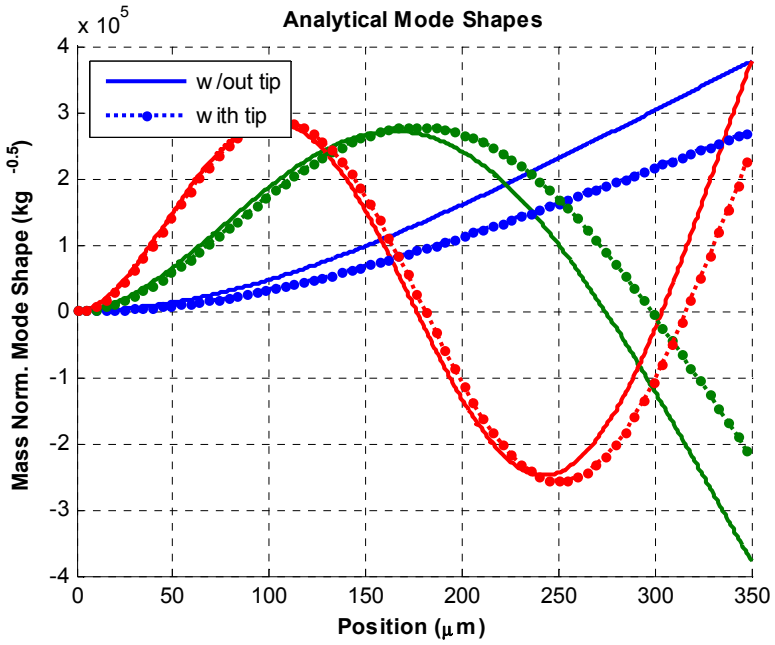

Figure 4: Analytically predicted mode shapes for cantilever AFM probes both without (solid) and with (dotted) a tip.

3.3. Effect on Calibration Methods

Using the value for the tip mass and tip location from the calibrated model discussed in the previous section, one can now use the corrected method of Sader in eqs. (4-5) to estimate the area density of the cantilever from the natural frequency and Q-factor measured in air. These were found to be 8969 kHz and 38.7 respectively for Beam 2. Values of 0.96 and 1.85e-5 were used for the density and viscosity of air. The former is a reasonable value for Albuquerque, NM, where the measurements were taken, and the latter is a nominal value. Considering the uncertainty in the measurement of the tip mass, two results are reported. The first, denoted "nominal tip", uses the tip mass estimated by SEM and using the nominal density for silicon, discussed earlier. The second uses the modified tip mass, found by tuning the Ritz model as described in the previous section. The results are shown in Table 4. The inclusion of the tip mass effect does not alter the prediction of the spring constant of the cantilever, for the reasons discussed earlier, but it does change the predicted area density by 34% and 130% respectively for the nominal tip mass and that found by tuning the Ritz model.

	Sader (no tip)	Modified Sader (nominal tip)	Percent Difference (nominal tip)	Modified Sader (tuned tip)	Percent Difference (tuned tip)
k_s	0.0424 N/m	0.0424 N/m	0 %	0.0424 N/m	0 %
$\rho_c h$	4.39 g/m^2	3.28 g/m^2	34%	1.90 g/m^2	130%

Table 4: Spring constants and area densities estimated using Sader's method and using the proposed approach that includes the effect of the tip mass.

The mode shapes from the tuned Ritz model were used to evaluate the effect that mode shape changes induced by the tip mass have on the method of Sader. The ratio of the true spring constant to the spring constant estimated by the Method of Sader was computed using eq. (6). This was found to be 0.996, 1.13 and 1.06 for the first, second and third modes of the cantilever respectively. Hence, one would expect errors of 0.4%, 13% and 6% respectively when using the first, second and third modes of the cantilever in the calibration procedure due to the fact that the probe's true mode shapes are different from the analytical. The error is small if the first mode is used because the shape of the first mode did not change shape appreciably. However, the experimentally measured shape of the 1st mode of Beam 1 was significantly different, so significant errors could be incurred when trying to calibrate Beam 1 using the Method of Sader.

4. Conclusions

This work has evaluated the effect of a probe tip on calibration by the method of Sader. The thermal tune method was found to produce similar results, although the specifics of that method were not discussed in detail. The method of Sader was modified to account for the mass of a probe tip, revealing that the area density estimated by that method can be significantly in error if the tip mass is not accounted for. The tip dimensions, found via SEM, were used to estimate the mass of the tip for the probe of interest, which was found to be 53% of the effective mass of the cantilever.

The spring constant estimated using the method of Sader was found to be unaffected by the tip mass, so long as the shape of the mode used in the calibration procedure was not altered by the presence of the tip. Experimental measurements of the natural mode shapes and of an AFM probe were obtained and compared with the analytical ones, verifying that little error is incurred in Sader's method if the first mode is used for calibration. Larger errors could occur for the higher modes. The errors were estimated to be 12% and 5% for the 2nd and 3rd modes respectively. Note however, that one of the AFM probes tested deviated significantly from the analytical model. The reason for this not known, yet it does suggest that other factors not modeled here could be important to the dynamics of the AFM probe, and hence have a significant effect on calibration. Future works should investigate this in light of the variability inherent in a batch of nominally identical probes, so that accurate quantitative results can be obtained with the AFM in a myriad of important applications.

The SEM estimate of the tip mass was used in a Ritz model for the AFM probe, yet it was was found to be insufficient to cause the observed changes in the mode shapes and frequencies of the AFM probe. We sought to estimate the mass of the tip of an AFM probe using an inverse dynamics procedure, adjusting the mass in a Ritz model until it agreed closely with the experiments. This process estimated the tip mass to be twice that estimated via SEM, or more than 120% of the effective mass of the beam. One should recall however, that it was necessary to assume that the stiffness of the cantilever, as estimated from the Q-factor by the method of Sader, was correct in order to estimate the absolute tip mass from the ratio of the tip mass to the beam mass ($m_t/(\rho_c bhL)$). The large discrepancy between the SEM and inverse dynamics estimated tip masses might be a result of inaccuracy in the spring constant estimated by the method of Sader. One would expect that the Q-factor estimated from vibration measurements would have an uncertainty of tens of percent or more, and this uncertainty is translated directly to the spring constant. If the spring constant were actually smaller, then the mass of the beam would be lower, and the tip-mass estimate would also be lower and closer to the SEM estimated value.

The inverse problem that must be solved to estimate the tip mass from the frequencies and mode shapes of the AFM probe is quite ill conditioned. There seem to be many combinations of the tip mass and tip location that provide some level of agreement. The uncertainties in the model, such as the non-uniformity of the beam, etc… seem to be significant enough to make finding a robust solution very difficult. Hence, the tip mass is not easy to estimate. On the other hand, it has a significant effect on the dynamics of the AFM probe, so some effort should at least be made.

5. Acknowledgements

The financial support provided by Sandia National Laboratories for this research is greatly appreciated. The authors also wish to thank Brandon Miller for his assistance in acquiring the SEM images of the cantilevers.

References

[1] R. Garcia and R. Perez, "Dynamic atomic force microscopy methods," *Surface Science Reports,* vol. 47, pp. 197-301, 2002.

[2] J. E. Sader, I. Larson, P. Mulvaney, and L. R. White, "Method for the calibration of atomic force microscope cantilevers," *Review of Scientific Instruments,* vol. 66, p. 3789, 1995.

[3] J. E. Sader, J. W. M. Chon, and P. Mulvaney, "Calibration of rectangular atomic force microscope cantilevers," *Review of Scientific Instruments,* vol. 70, pp. 3967-9, 1999.

[4] J. L. Hutter and J. Bechhoefer, "Calibration of atomic-force microscope tips," *Review of Scientific Instruments,* vol. 64, pp. 1868-73, 1993.

[5] T. J. Senden and W. A. Ducker, "Experimental determination of spring constants in atomic force microscopy," *Langmuir,* vol. 10, pp. 1003-1004, 1994.

[6] M. Tortonese and M. Kirk, "Characterization of application specific probes for SPMs," San Jose, CA, USA, 1997, pp. 53-60.

[7] J. P. Cleveland, S. Manne, D. Bocek, and P. K. Hansma, "A nondestructive method for determining the spring constant of cantilevers for scanning force microscopy," *Review of Scientific Instruments,* vol. 64, pp. 403-5, 1993.

[8] S. Crittenden, A. Raman, and R. Reifenberger, "Probing attractive forces at the nanoscale using higher-harmonic dynamic force microscopy," *Physical Review B (Condensed Matter and Materials Physics),* vol. 72, pp. 235422-1, 2005.
[9] J. E. Sader, "Frequency response of cantilever beams immersed in viscous fluids with applications to the atomic force microscope," *Journal of Applied Physics,* vol. 84, pp. 64-76, 1998.
[10] J. H. Ginsberg, *Mechanical and Structural Vibrations*, First ed. New York: John Wiley and Sons, 2001.
[11] J. Melcher, S. Hu, and A. Raman, "Equivalent point-mass models of continuous atomic force microscope probes," *Applied Physics Letters,* vol. 91, p. 053101, 2007.
[12] J. H. Ginsberg, *Advanced Engineering Dynamics*, 2nd ed. Cambridge, UK: Cambridge University Press, 1998.
[13] M. Allen, H. Sumali, and D. Epp, "Piecewise-linear restoring force surfaces for semi-nonparametric identification of nonlinear systems," *Nonlinear Dynamics,* 2007.